

1 **Supplemental Material for**

2
3 **Three pairs of surrogate redox partners comparison for Class I cytochrome P450 enzyme activity**
4 **reconstitution**

5
6 Xiaohui Liu^{1†}, Fengwei Li^{1†}, Tianjian Sun¹, Jiawei Guo¹, Xingwang Zhang^{1,2}, Xianliang Zheng³, Lei
7 Du¹, Wei Zhang¹, Li Ma^{1*}, Shengying Li^{1,2}

8
9 ¹State Key Laboratory of Microbial Technology, Shandong University, Qingdao, Shandong 266237,
10 China.

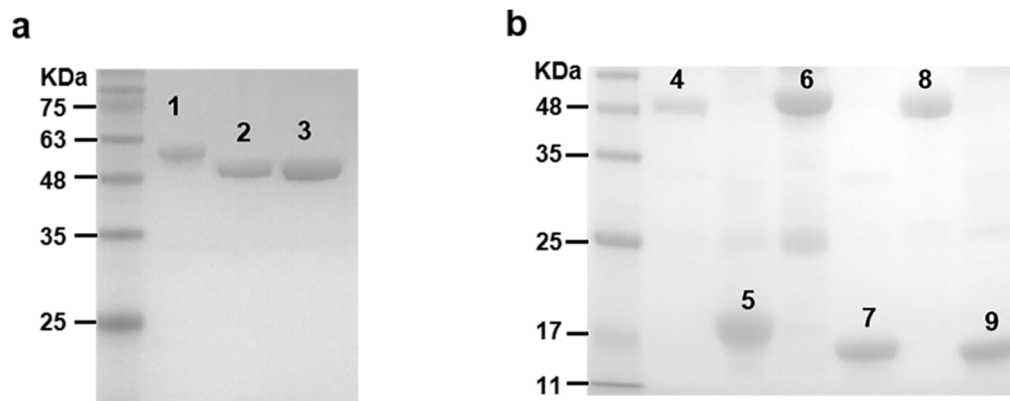
11 ²Laboratory for Marine Biology and Biotechnology, Qingdao National Laboratory for Marine Science
12 and Technology, Qingdao, Shandong 266237, China.

13 ³Center For Biocatalysis and Enzyme Technology, AngelYeast Co., Ltd., Cheng Dong Avenue,
14 Yichang, Hubei, 443003, China

15
16 *Corresponding Author E-mail: maliqd@sdu.edu.cn

17 †These authors contributed equally.

18

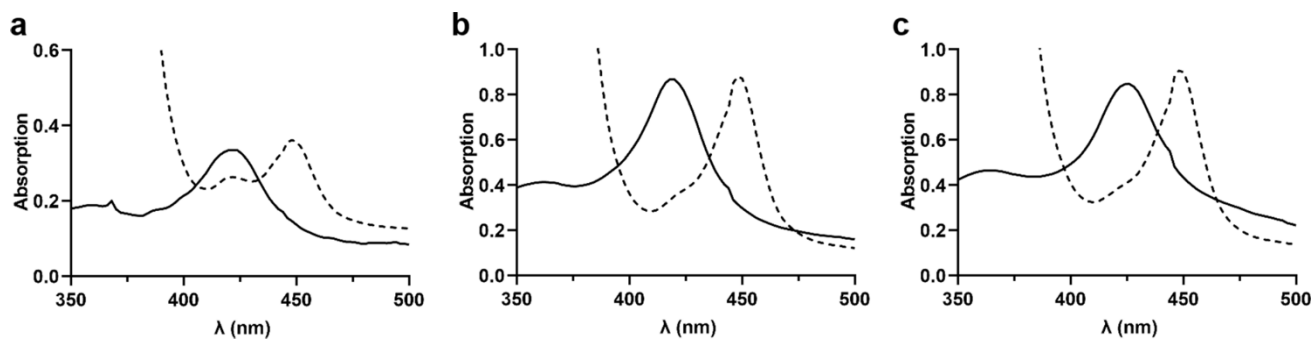


19

20 **Supplementary Fig 1.** SDS-PAGE analysis of purified cytochrome P450s (a) and redox partners (b).

21 Lane 1, CYP-sb21; 2, P450sca-2; 3, PikC; 4, *SelFdr0978*; 5, *SelFdx1499*; 6, AdR; 7, Adx; 8, PdR; 9,

22 Pdx. Proteins were stained with Coomassie blue in 12.5% polyacrylamide gel.



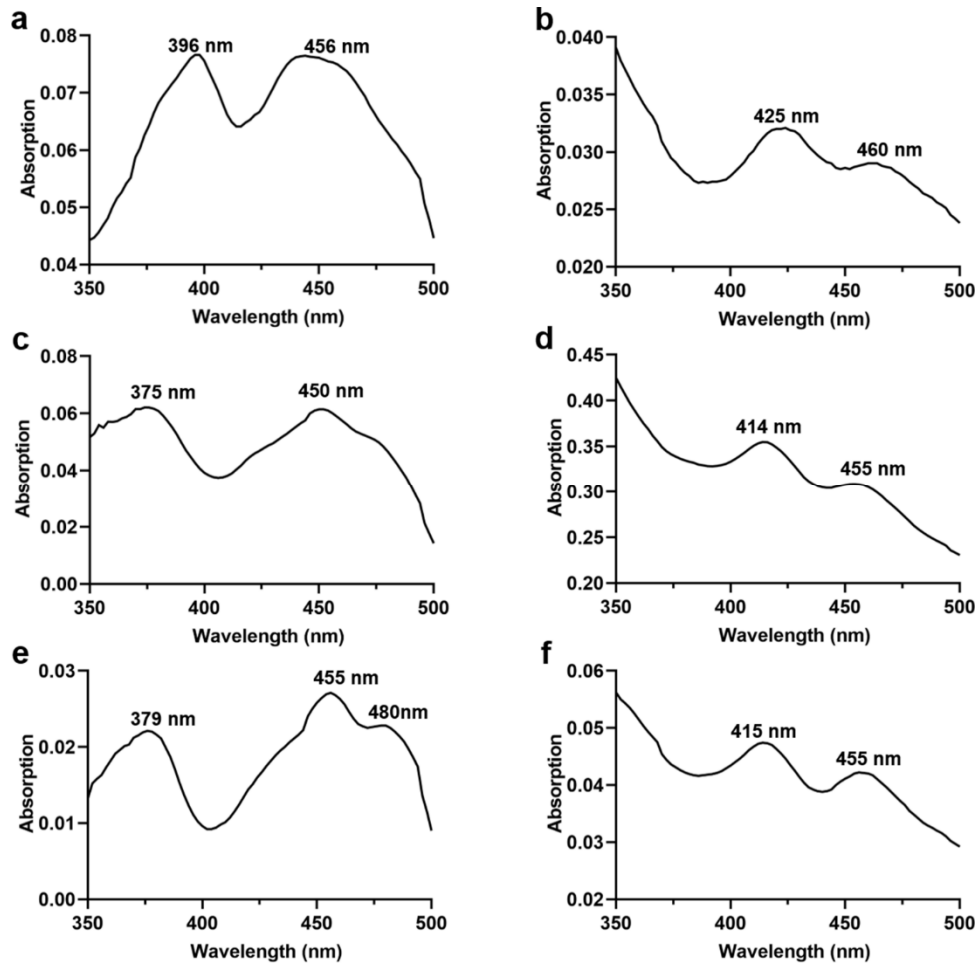
23

24 **Supplementary Fig 2.** CO-bound reduced difference spectra of purified P450s. (a) PikC, (b) P450sca-

25 2, (c) CYP-sb21. *Dotted line*, P450 absorbance spectra in ferrous CO-complexed state; *Solid line*, ferric

26 state. This assay was also employed to determine the concentrations of functional cytochrome P450

27 enzymes using the extinction of $91,000 \text{ M}^{-1}\text{cm}^{-1}$ ^{1,2}.

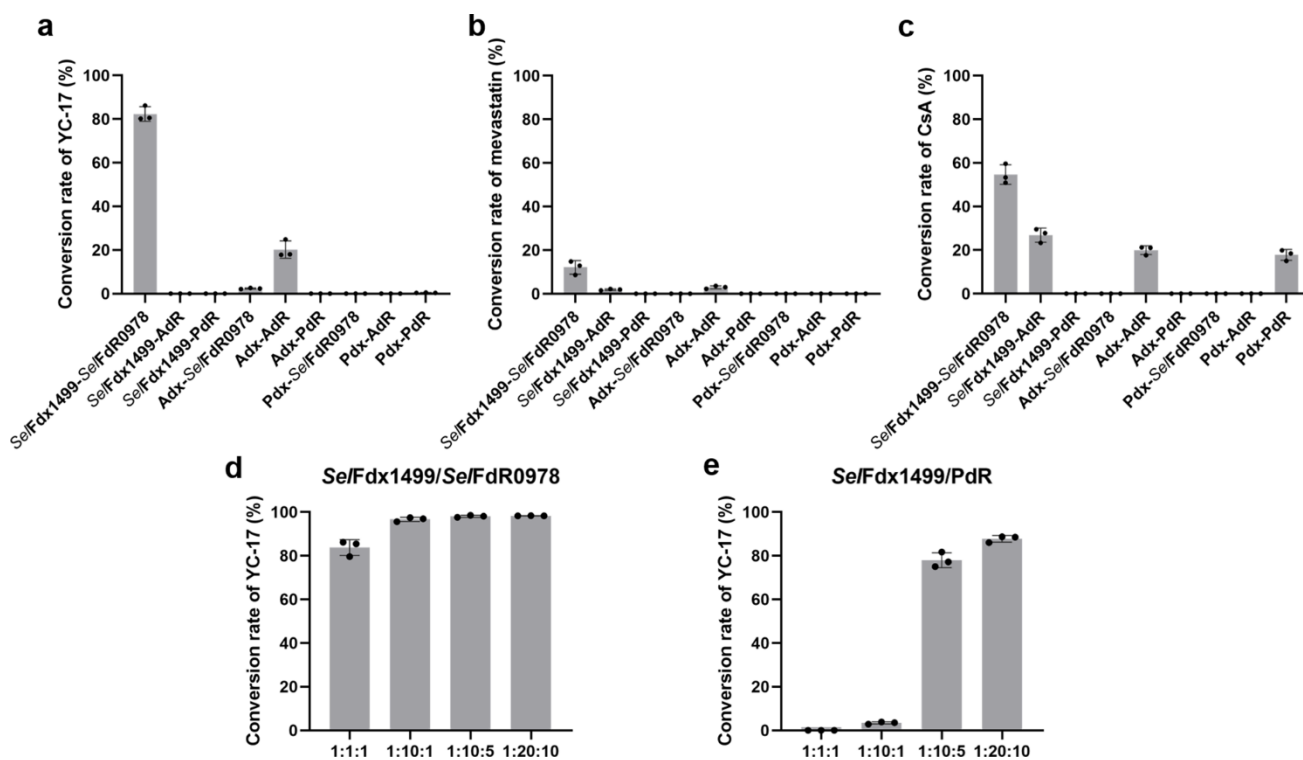


28

29 **Supplementary Fig 3.** UV/Vis absorption spectra of the selected redox partner proteins. (a)

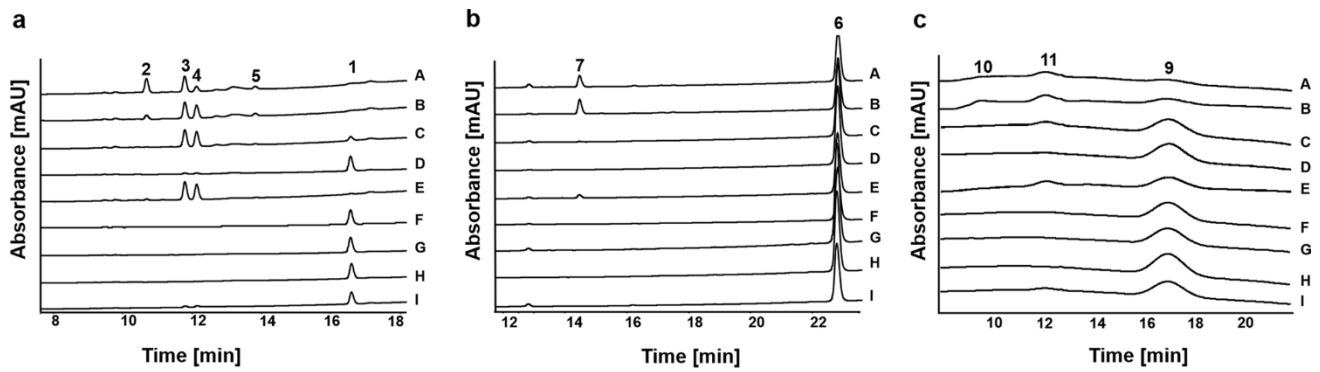
30 *Se/FdR0978*, (b) *Se/Fdx1499*, (c) AdR, (d) Adx, (e) PdR, and (f) Pdx.

31



32

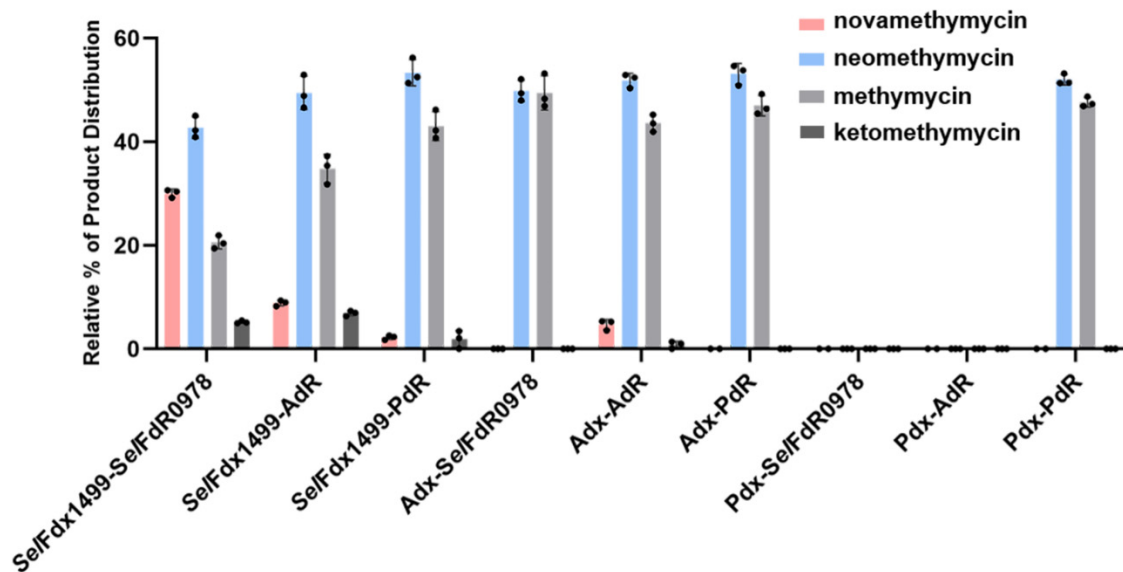
33 **Supplementary Fig 4.** The effects of different P450/Fdx/FdR ratios on P450-mediated catalysis. The
 34 catalytic activities of PikC (a), P450sca-2 (b), and CYP-sb21 (c) when supported by an equal molar
 35 ratio of P450, Fdx and FdR. The catalytic activities of PikC when supported by different ratios of
 36 *Se/Fdx1499/Se/FdR0978* (d) and *Se/Fdx1499/PdR* (e). All the experiments were carried out in
 37 triplicate. The error line represents the standard deviation. *P* values in each groups were calculated
 38 with single factor ANOVA analysis, and all *P* values were less than 0.01.



39

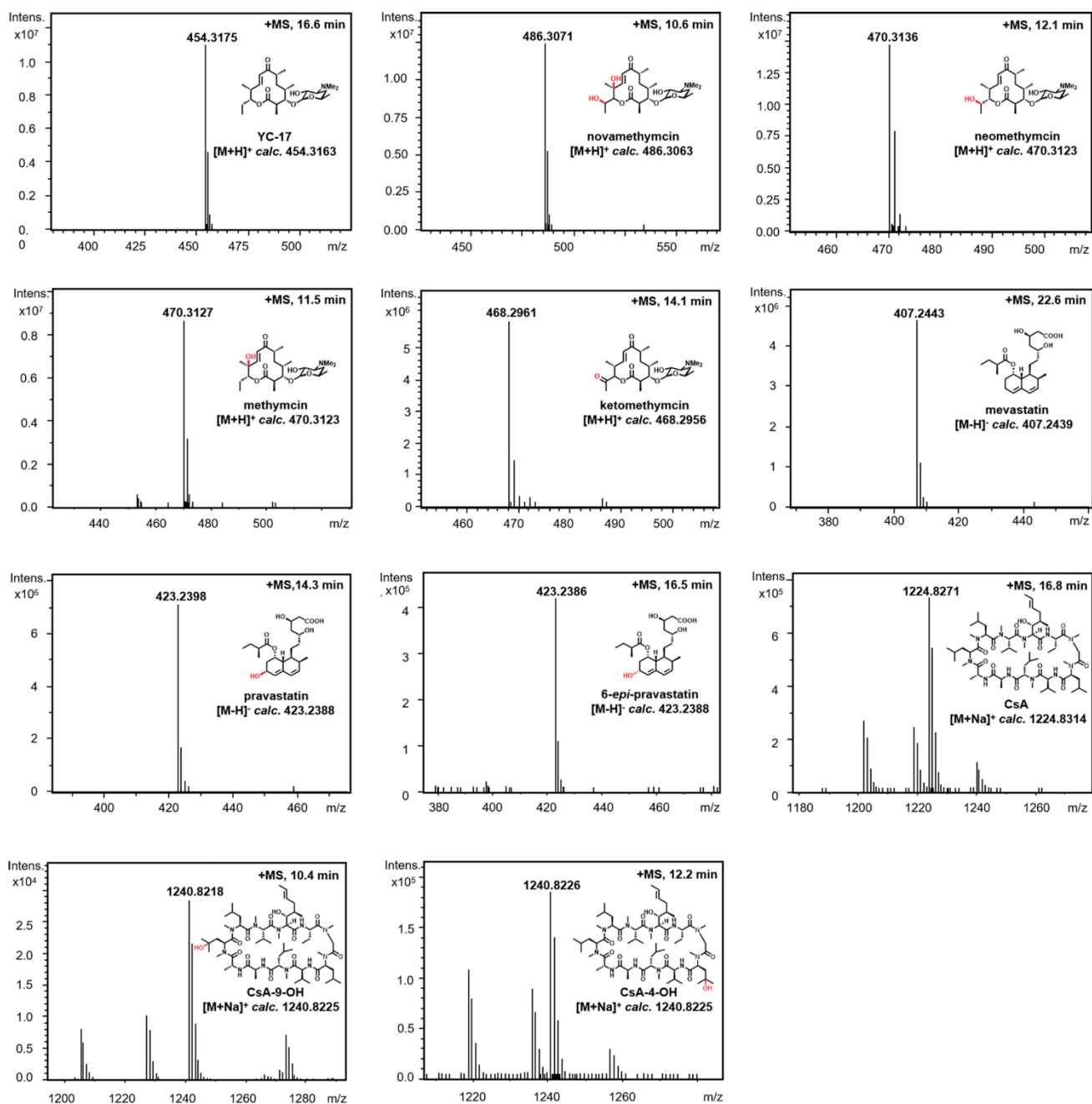
40 **Supplementary Fig 5.** HPLC analysis of three P450 enzymatic reactions. (a) PikC hydroxylates YC-
 41 17 (**1**) at either C10 or C12 position, giving rise to neomethymycin (**3**), methymycin (**4**),
 42 novamethymycin (**2**), and ketomethymycin (**5**). (b) P450sca-2 converts mevastatin (**6**) into pravastatin
 43 (**7**). (c) CYP-sb21 hydroxylates CsA (**9**) into CsA-9-OH (**10**) and/or CsA-4-OH (**11**) to different extents.
 44 A, *Se*/Fdx1499/*Se*/FdR0978; B, *Se*/Fdx1499/AdR; C, *Se*/Fdx1499/PdR; D, Adx/*Se*/FdR0978; E,
 45 Adx/AdR; F, Adx/PdR; G, Pdx/*Se*/FdR0978; H, Pdx/AdR; I, Pdx/PdR.

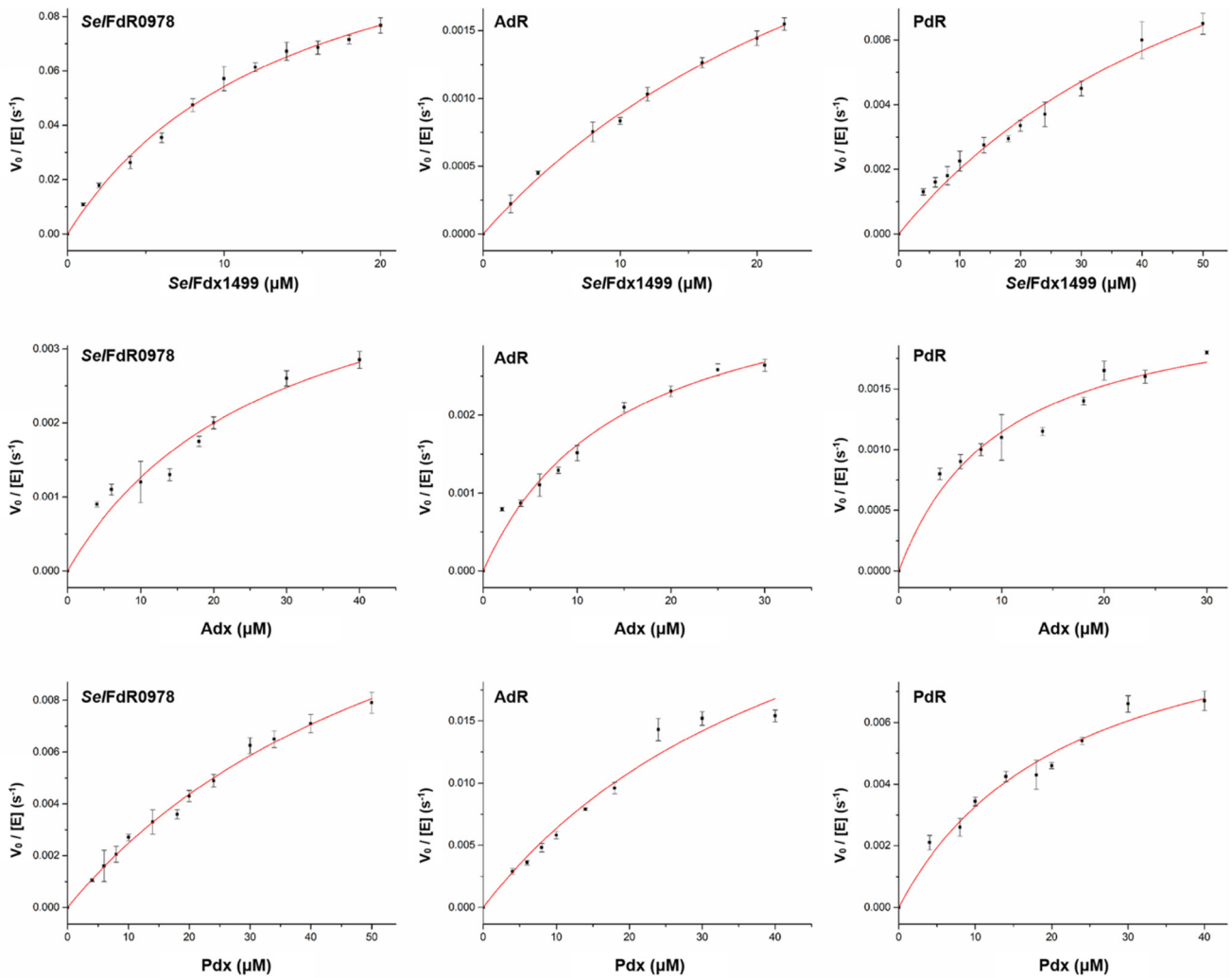
46



47

48 **Supplementary Fig 6.** Products distribution of PikC when coupled with 9 different combinations of
 49 redox partners. The diagram shows the relative percentage of products (%) obtained from the *in vitro*
 50 conversions of YC-17 by PikC in the presence of GDH/glucose as NAD(P)H recycling system. The
 51 error line represents the standard deviation. *P* values in each groups were calculated with single factor
 52 ANOVA analysis, and all *P* values were less than 0.01.

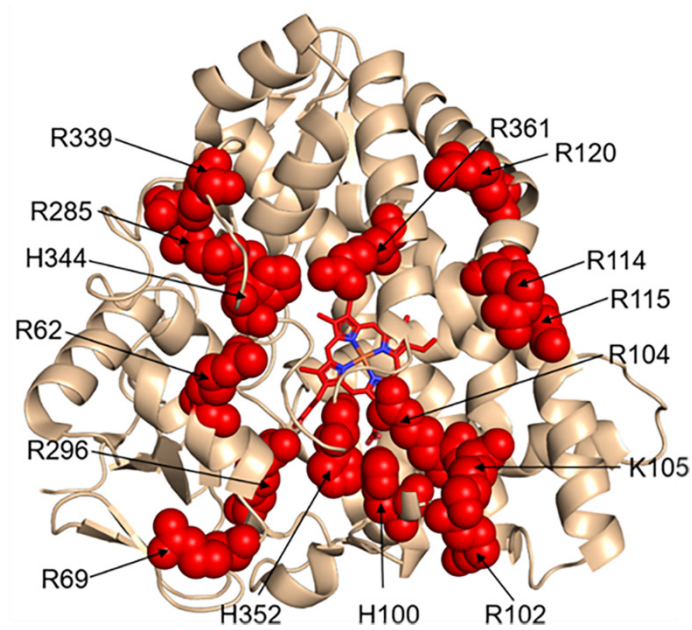




56

57 **Supplementary Fig 8.** The steady-state kinetic curves of cytochrome *c* (cyt *c*) reduction by 9 pairs of
 58 redox partners. In the electron transfer assays, cyt *c* was used as the final electron acceptor. The assays
 59 were carried out on a SpectraMax M2 plate reader (USA) at 30 °C by varying the concentrations of
 60 Fdxs in 50 mM sodium phosphate buffer (pH 7.4).

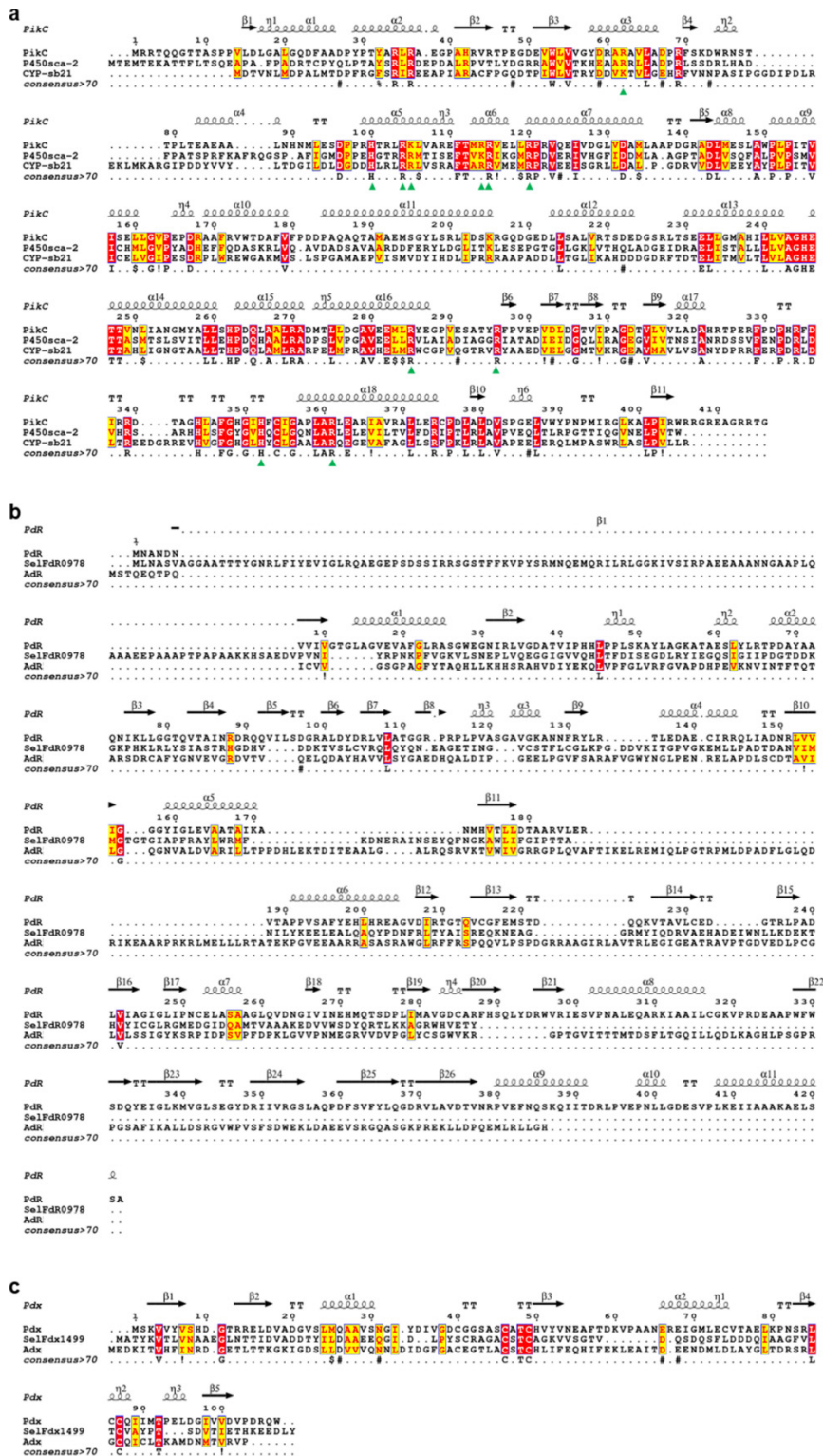
61



62

63 **Supplementary Fig 9.** The conservative basic amino acids on the proximal surface of the three P450
64 enzymes. Basic amino acids R, H or K in different P450s were mapped onto the proximal surface of
65 PikC, which form a conservative positively charged surface.

66



67

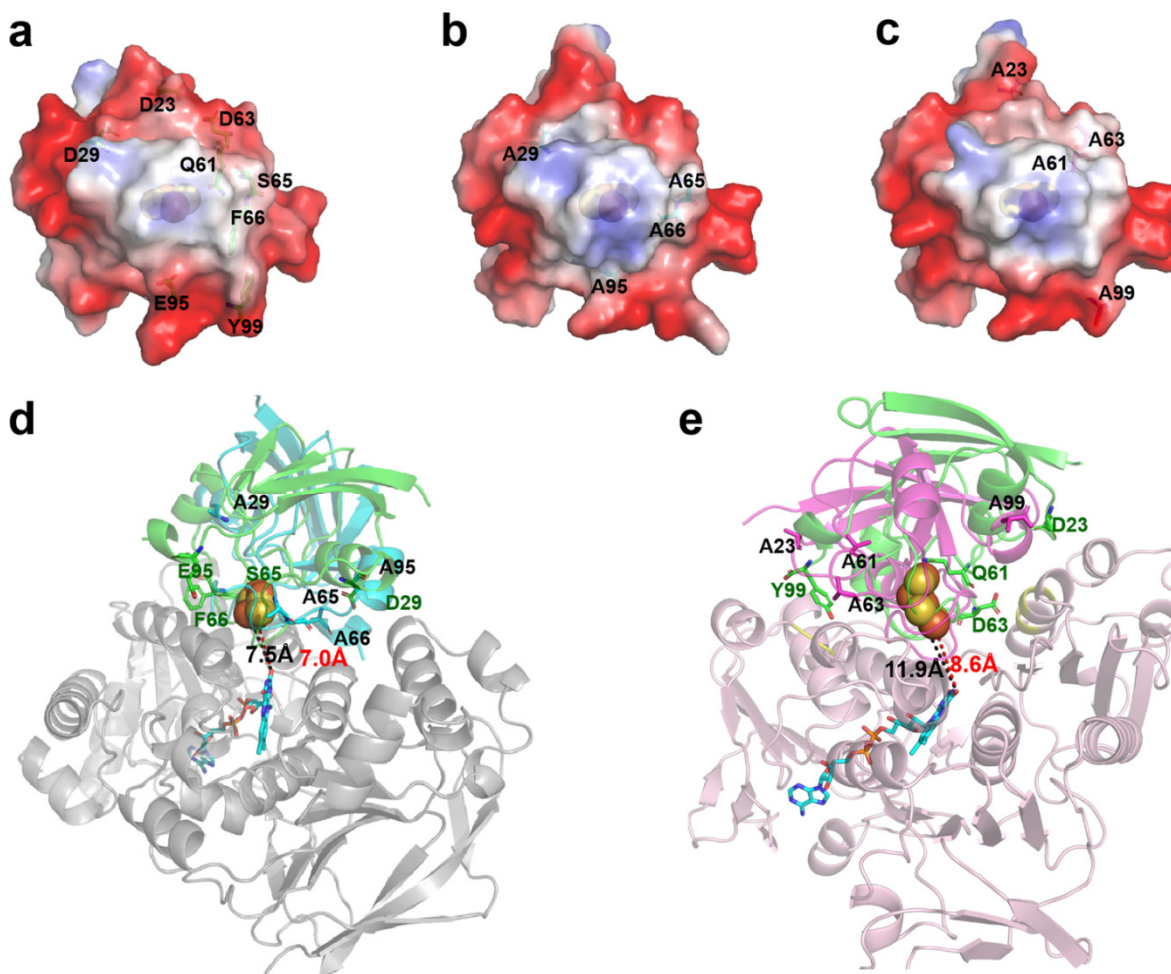
68 **Supplementary Fig 10.** Protein sequence alignment of the studied P450s (a), Fdxs (b) and FdRs (c).

69 The secondary structure alignments are based on the models of PikC (PDB ID: 2BVJ), PdR (PDB ID:

70 1Q1R), and Pdx (PDB ID: 1VJI). The conservative basic amino acids R, H and K on the proximal

71 surface of P450s are stamped by green triangles. Sequence alignment based on their tertiary structures

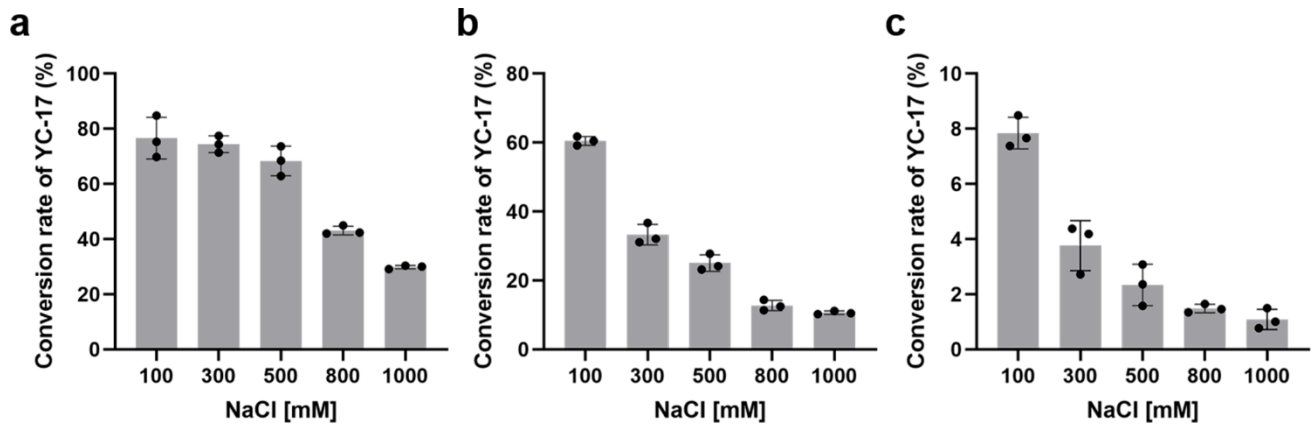
72 was prepared using T-COFFEE online service^{3,4} and the figure was output by ESPrnt 3.0⁵.



73

74 **Supplementary Fig 11.** The electrostatic surface and interface analysis of AdR-*SeIFdx1499*, and PdR-
 75 *SeIFdx1499* before and after mutagenesis. The electrostatic surface analysis of *SeIFdx1499* (a),
 76 *SeIFdx1499*-M2 (b), and *SeIFdx1499*-M3 (c). Positively and negatively charged surfaces are colored
 77 in blue and red, respectively. Docking models of *SeIFdx1499* mutants in complex with AdR (d) and
 78 PdR (e). The wild-type *SeIFdx1499* is shown in green and the key interacting residues on AdR/PdR-
 79 *SeIFdx1499* interfaces are shown as sticks. When replaced by alanine, the mutant *SeIFdx1499* coupled
 80 with AdR or PdR is shown in cyan (d) and pink (e). FAD is shown as sticks in cyan. The Fe₂S₂ cluster
 81 is shown as spheres. The shortest FAD-Fe₂S₂ distances (Å) of wide-type and mutant-type are indicated
 82 by black and red dashed lines, respectively.

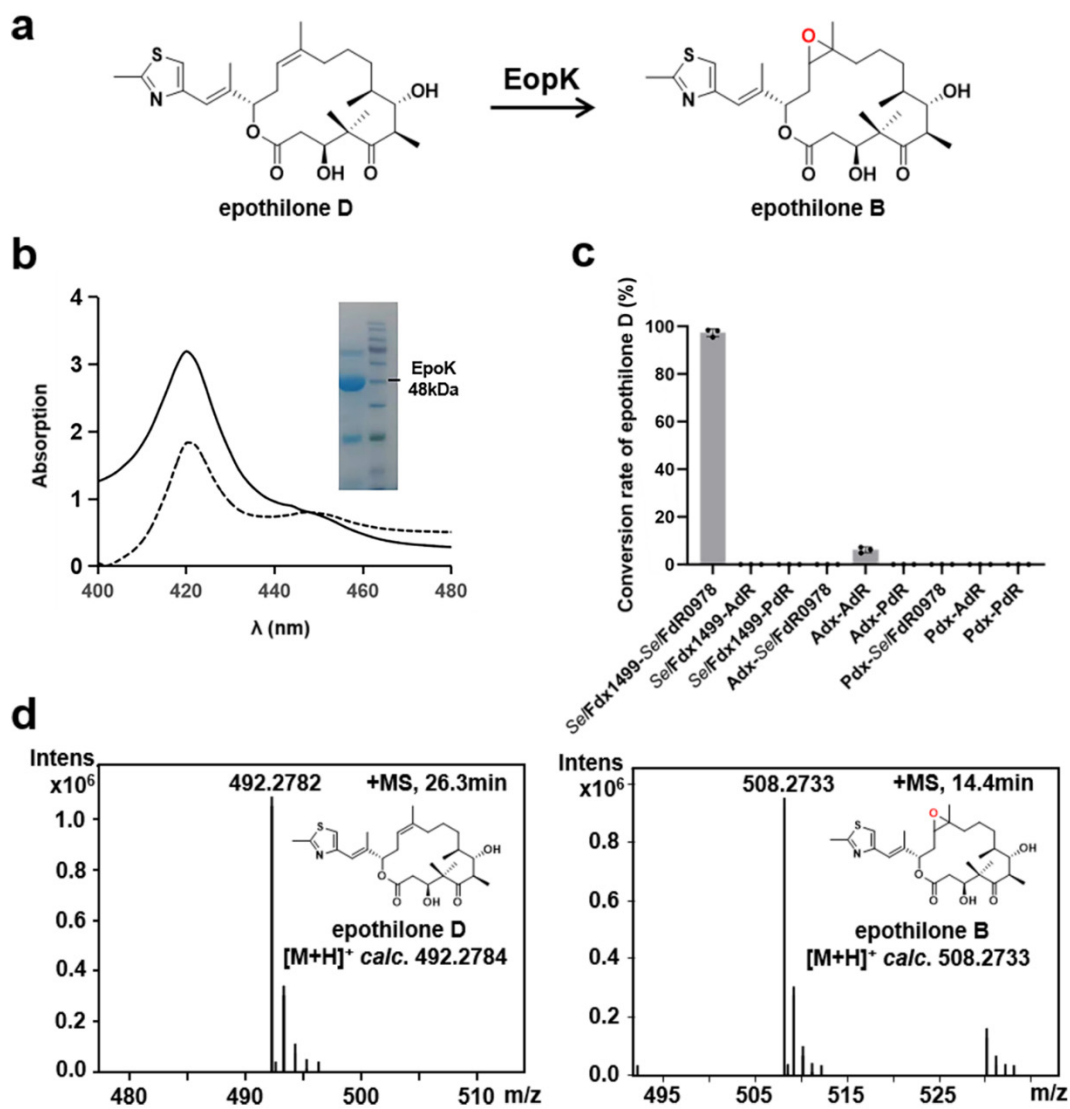
83



84

85 **Supplementary Fig 12.** Conversions of YC-17 by *PikC/Se/Fdx1499/Se/FdR0978* (a), *PikC/Adx/AdR*
 86 (b), and *PikC/Pdx/PdR* (c) under different NaCl concentrations. All the experiments were carried out
 87 in triplicate. $P < 0.01$, P-value was calculated with single factor ANOVA analysis. The error line
 88 represents the standard deviation. *P* values in each groups were calculated with single factor ANOVA
 89 analysis, and all *P* values were less than 0.01.

90



91

92 **Supplementary Fig 13.** Conversion of epothilone D to B catalyzed by EpoK. (a) The EpoK-catalyzed
 93 reaction. (b) The CO-bound reduced difference spectrum of purified EpoK. (c) The catalytic activities
 94 of EpoK when supported by nine different combinations of redox partners. (d) High resolution mass
 95 spectra of the substrate and product associated with the EpoK-mediated reaction.

96 **Supplementary Table 1.** Coupling efficiency for 9 redox partner pairs measured with PikC, P450sca-
 97 2 and CYP-sb21. “-” means no product was detected.

	PikC	P450sca-2	CYP-sb21
	Coupling efficiency (%)	Coupling efficiency (%)	Coupling efficiency (%)
<i>Se/Fdx1499/Se/FdR0978</i>	85.6 ± 2.1	86.4 ± 5.3	12.6 ± 1.8
<i>Se/Fdx1499/AdR</i>	76.1 ± 1.8	4.8 ± 0.9	3.2 ± 0.5
<i>Se/Fdx1499/PdR</i>	9.4 ± 1.7	14.9 ± 2.2	1.2 ± 0.5
<i>Adx/Se/FdR0978</i>	16.4 ± 0.2	-	-
<i>Adx/AdR</i>	83.1 ± 3.2	20.1 ± 1.3	5.0 ± 2.3
<i>Adx/PdR</i>	9.4 ± 6.7	-	-
<i>Pdx/Se/FdR0978</i>	-	-	-
<i>Pdx/AdR</i>	-	-	-
<i>Pdx/PdR</i>	72.4 ± 4.0	-	3.3 ± 0.4

98

99 **Supplementary Table 2.** Strains and plasmids used in this study.

<i>E. coli</i> strain or plasmid	Relevant characteristics	Reference/Source
Strains		
DH5 α	Cloning host	Life Technologies
BL21(DE3)	Expression host	Life Technologies
Plasmids		
pET28b- <i>pikC</i>	Plasmid pET28b harboring <i>pikC</i> gene	Wei Zhang et al. ⁶
pET28b- <i>P450sca-2</i>	Plasmid pET28b harboring <i>P450sca-2</i> gene	Wei Zhang et al. ⁶
pET28b- <i>cyp-sb21</i>	Plasmid pET28b harboring <i>cyp-sb21</i> gene	Li Ma et al. ⁷
pET28b- <i>selfdR0978</i>	Plasmid pET28b harboring <i>selfdR0978</i> gene	Li Ma et al. ⁷
pET28b- <i>selfdx1499</i>	Plasmid pET28b harboring <i>selfdx1499</i> gene	Li Ma et al. ⁷
pCwori ⁺ - <i>adR</i>	Plasmid pCwori ⁺ harboring <i>adR</i> (4-108) gene, added His-tag	This work
pET30a- <i>adx</i>	Plasmid pET30a harboring <i>adx</i> gene, added His-tag	This work
pET28b- <i>pdx</i>	Plasmid pET28b harboring <i>pdx</i> gene	Wei Zhang et al. ⁶
pET19b- <i>pdR</i>	Plasmid pET19b harboring <i>pdR</i> gene	Wei Zhang et al. ⁶
pET28b- <i>selfdx1499-M1-M4</i>	Plasmid pET28b harboring <i>selfdx1499-M1-M4</i> gene	This work
pET30a- <i>adx-M1-M4</i>	Plasmid pET30a harboring <i>adx-M1-M4</i> gene	This work
pET28b- <i>pdx-M1-M4</i>	Plasmid pET28b harboring <i>pdx-M1-M4</i> gene	This work

101 **Supplementary Table 3.** Primers used in this study

Oligonucleotide	Primer sequence (5'-3')	Function of underlined bases
Adx-F	CGGGGT <u>ACCAT</u> GGAAGATAAAATAACAGTCC	<i>Kpn</i> I restriction site
Adx-R	CCCTCGAGT <u>TAAAG</u> TACTCGAACAGTC	<i>Xho</i> I restriction site
AdR-F	GGAATTCC <u>CATATG</u> AGCACTCAAGAACAACACTC	<i>Nde</i> I restriction site
AdR-R	CCCTCGAGGTGCCCCAGCAGCCGCAGCA	<i>Xho</i> I restriction site

102

103 **Supplementary References**

- 104 1 Li, S., Podust, L. M. & Sherman, D. H. Engineering and analysis of a self-sufficient
105 biosynthetic cytochrome P450 PikC fused to the RhFRED reductase domain. *J. Am. Chem. Soc.*
106 **129**, 12940-12941 (2007).
- 107 2 Omura, T. & Sato, R. The carbon monoxide-binding pigment of liver microsomes. II.
108 solubilization, purification, and properties. *J. Biol. Chem.* **239**, 2379-2385 (1964).
- 109 3 Notredame, C., Higgins, D. G. & Heringa, J. T-Coffee: A novel method for fast and accurate
110 multiple sequence alignment. *J. Mol. Biol.* **302**, 205-217 (2000).
- 111 4 Di Tommaso, P. *et al.* T-Coffee: a web server for the multiple sequence alignment of protein
112 and RNA sequences using structural information and homology extension. *Nucleic Acids Res.*
113 **39**, W13-17 (2011).
- 114 5 Robert, X. & Gouet, P. Deciphering key features in protein structures with the new ENDscript
115 server. *Nucleic Acids Res.* **42**, W320-324 (2014).
- 116 6 Zhang, W. *et al.* Mechanistic insights into interactions between bacterial class I P450 enzymes
117 and redox partners. *ACS Catal.* **8**, 9992-10003 (2018).
- 118 7 Ma, L. *et al.* Reconstitution of the *in vitro* activity of the cyclosporine-specific P450
119 hydroxylase from *Sebekia benihana* and development of a heterologous whole-cell
120 biotransformation system. *Appl. Environ. Microbiol.* **81**, 6268-6275 (2015).
- 121